Anomalous diffusion in the nonasymptotic regime

C. A. Condat,[1,2] J. Rangel,[1] and Pedro W. Lamberti[2]
[1]*Department of Physics, University of Puerto Rico, Mayagüez, Puerto Rico 00681*
[2]*Facultad de Matemática, Astronomía y Física, Universidad Nacional de Córdoba, Ciudad Universitaria, 5000 Córdoba, Argentina, and CONICET, Argentina*

(Received 9 August 2001; published 24 January 2002)

We analyze some properties of the one-dimensional Lévy flights, assuming that the one-step transition rates depend on the flight length x as $p_\alpha(x) \sim x^{-(\alpha+2)}$. For flights on a finite, $(2M+1)$-site lattice, we can define an effective, size-dependent, diffusion coefficient $D_\alpha(M) \sim [M^{1-\alpha}-1]/(1-\alpha)$ if $\alpha<1$, with $D_1(M) \sim \ln(M)$. Using the generalization of statistical mechanics given by Tsallis, we show that for flights on infinite systems, the generalized displacement moments $\langle x^R \rangle$ are well defined provided that $\alpha > R-3$. These moments exhibit a power-law singularity if $\alpha \to 1^-$ and $R>2/3$. The short- and intermediate-time properties of the generalized mean-square displacement are then studied numerically. This work suggests the conditions under which the asymptotic analytical formulas (obtained in the literature by the use of the generalized central limit theorem) could be applied to finite-time experiments. These formulas should work much better if α is close to zero than in the $\alpha \to 1^-$ neighborhood.

DOI: 10.1103/PhysRevE.65.026138 PACS number(s): 02.50.Ey, 05.40.−a

I. INTRODUCTION

The beauty of the concept of Lévy flights has attracted the attention of mathematicians and theorists for many years [1], but it has been only recently that it has proved useful to further our understanding of experimental situations [2–14]. A distinctive feature of Lévy flights is the divergence of the displacement moments. In practical problems this divergence may be eliminated by either considering a finite diffusion domain (truncated Lévy flights have been successfully used to model market fluctuations [9,11]), or assuming that the flyer has a finite translational speed. This last case is often referred to as a ''Lévy walk,'' and has been exhaustively studied by Weeks, Urbach, and Swinney [6,7]. A new way of looking at the moments has been recently introduced by workers that applied Tsallis' nonextensive statistical mechanics (TNSM) [15–17]. TNSM has been fruitfully used in a host of physical problems [18–20]. In particular, the resulting nonextensive thermodynamics has shed new light on problems involving long-range interactions [21]. Despite these successes, however, no causal connection has yet been found, in general, between the value of the parameter q that characterizes Tsallis' theory and the properties of the long-range interactions. Therefore, the only test of the validity of the theory remains its ability to correctly explain and predict experimental results, while q is often used only as a fitting parameter [22].

The papers by Zanette and Alemany [15] and by Tsallis, Levy, Souza, and Maynard [16] showed that it is possible to use the TNSM to consistently define the second moment of the displacement for Lévy flights. This is an interesting development, not only because concrete predictions can be made, but also because the value of q can be directly related to the flight properties. Thus, the interplay between TNSM and Lévy flights may not only open the way to a better understanding of the connections between Lévy flights and physical reality but they may also help us to strengthen the foundations of the TNSM.

It is clear that precise, reliable predictions are needed in order to either verify or falsify the TNSM. For this reason, it seems appropriate to perform a careful study for a model as simple as possible of a Lévy flight using the ideas of Tsallis. In this paper we analyze an elementary model for a Lévy flight on a lattice, obtaining concrete predictions for the generalized displacements. Due to computational requirements, our numerical work is necessarily restricted to the short- and intermediate-time regimes. But it is precisely these regimes that are usually accessible to the experimentalist. Furthermore, our analysis completes the picture presented in Ref. [16], where the generalized central limit theorem was used to investigate the large jump number (i.e., the long-time) limit. Our calculations show that, for certain values of the parameters, the range of validity of the dependence of the mean-square displacement on jump number obtained in Ref. [16] can be extended to finite times. They also indicate that there is a parameter region in which marked differences arise between the short- and long-time forms. We will suggest an explanation for this behavior.

The rest of this paper is organized as follows: In Sec. II we summarize the results predicted by the standard theory for long-jump diffusion in finite and infinite lattices. In Sec. III, we review the application of TNSM to anomalous diffusion and discuss some properties of the generalized displacement moments. In Sec. IV we investigate the mean-square displacement numerically. We start with a brief explanation of the methods used in the simulations and then examine the results. The paper closes in Sec. V with the conclusions and some suggestions for future work.

II. STANDARD DIFFUSION: ANALYTICAL RESULTS

A. Long jumps on an infinite lattice

First, consider an infinite one-dimensional lattice. For simplicity, we will take the lattice constant to be unity. A particle is deposited at the origin at time $t=0$ and is allowed to jump to any other lattice site; the jump rates to the left and

to the right will be denoted by Λ_k and Γ_k, respectively, where k, a positive integer, is the distance between the departure and arrival sites. The system is assumed to be homogeneous, i.e., the jump rates do not depend on the location of the departure site. The probability $P_j(t)$ that the jth site is occupied at time t can be obtained from the master equation

$$\dot{P}_j(t)=\sum_{k>0}\left[\Gamma_k(P_{j-k}-P_j)+\Lambda_k(P_{j+k}-P_j)\right], \quad (2.1)$$

subject to the initial condition $P_j(0)=\delta_{j,0}$.

The displacement moments can be calculated using the generating function

$$G(t,z)=\sum_{j=-\infty}^{\infty} z^j P_j(t), \quad (2.2)$$

which satisfies $G(0,z)=1$. Taking the time derivative of G and using Eq. (2.1), we find

$$G(t,z)=\exp\left\{t\sum_{k>0}\left[\Gamma_k z^k+\Lambda_k z^{-k}-(\Gamma_k-\Lambda_k)\right]\right\}. \quad (2.3)$$

The displacement moments are now

$$\langle x^n(t)\rangle=\left[\left(z\frac{\partial}{\partial z}\right)^n G(t,z)\right]_{z=1}. \quad (2.4)$$

Of course, these quantities are well defined only as long as all series involved converge. If this is the case, it is easy to show that $\langle x(t)\rangle=Vt$ and $\langle x^2(t)\rangle-\langle x(t)\rangle^2=2Dt$, where the drift velocity V and the diffusion coefficient D are given by

$$V=\sum_{k>0}(\Gamma_k-\Lambda_k)k \quad (2.5)$$

and

$$D=\frac{1}{2}\sum_{k>0}(\Gamma_k+\Lambda_k)k^2. \quad (2.6)$$

Next we analyze the convergence. Assuming, for simplicity, that $\Gamma_k\geqslant\Lambda_k$ for large k, it suffices to consider jumps to the right. If $\Gamma_k\sim k^{-(2+\alpha)}$ for large k, probability normalization demands that $\alpha>-1$. Depending on the value of α we have three regimes. (i) $-1<\alpha<0$, neither V nor D is well defined; (ii) $0<\alpha<1$, V is well defined but D is not; and (iii) $1<\alpha$, normal diffusion.

In the remainder of this work, we consider only symmetric jump probability distributions such that $\Lambda_k=\Gamma_k$ and $V=0$. We also choose $\Gamma_k=\gamma_\alpha k^{-(2+\alpha)}$. By normalizing the jump probability distribution, we find $\gamma_\alpha=[2\zeta(2+\alpha)]^{-1}$, where $\zeta(\alpha)=\Sigma_{k=1}k^{-\alpha}$ is Riemann's zeta function [23]. In the normal diffusion regime, $\alpha>1$, the diffusion coefficient is then given by

$$D_\alpha=\frac{\zeta(\alpha)}{2\zeta(2+\alpha)}. \quad (2.7)$$

Note that in the $\alpha\to\infty$ limit, $\Gamma_k=0.5\delta_{k,1}$, we recover the usual random walk result, $D_\infty=1/2$. If $\alpha\to1^+$, on the other hand, the diffusion coefficient diverges.

B. Long jumps on a finite lattice

What happens if long jumps are allowed but the diffusion space is finite? The finite lattice problem with long jumps is not only interesting in itself (all real lattices are finite), but it is also the one we actually investigate using numerical simulations. In this context, we note that few years ago, Mantegna and Stanley studied the slow convergence of truncated Lévy flights to the Gaussian attractor [24]. A numerical analysis using a finite lattice can give useful information about diffusion on infinite lattices if we restrict the processes to shorter times compared with $\hat{t}_M$, a time for which a non-negligible proportion of the particles in the ensemble have reached the boundaries. This characteristic time will depend not only on the form of the distribution Γ_k and on the number $(2M+1)$ of lattice sites, but also on the order of the moment we are calculating: The weight of distant particles increases for higher moments, which reduces the value of $\hat{t}_M$. For times shorter than $\hat{t}_M$ the results should be independent of our choice of the boundary conditions (BC's). We will now obtain some results using reflecting BC's, where by ''reflecting'' we mean simply that jumps leading outside of the interval $[-M,M]$ are forbidden. The environment recorded by a jumping particle will then depend on the jump departure site.

By suitably restricting the sums in Eq. (2.6), we can calculate an effective ''local diffusion function,'' $D(M,j)$, which is the local equivalent of the standard diffusion coefficient for a particle located at a site $j\in[-M,M]$,

$$D(M,j)=\frac{1}{2}\left(\sum_{k=1}^{M-j}k^2\Gamma_k+\sum_{k=1}^{M+j}k^2\Gamma_k\right). \quad (2.8)$$

This dependence of D on the position is due to the truncation of the longest jumps, which is a function of the location of the site where the jump originates. The same truncation generates an effective local drift

$$V(M,j>0)=-\sum_{k=N-j+1}^{N+j}k\Gamma_k. \quad (2.9)$$

For sites $j<0$ the local drift is positive, satisfying $V(M,j<0)=-V(M,j>0)$. Of course, $V(M,0)=0$. The local drift is maximum near the lattice ends. Equations (2.8) and (2.9) can be also obtained by starting with the master equation for the finite system and then taking the continuum limit. Since we are considering finite lattices, these equations remain valid even if $\alpha\leqslant-1$.

For $t\ll\hat{t}_M$, it is enough to consider $j\ll M$. If $\Gamma_k\sim\gamma k^{-(2+\alpha)}$, this immediately yields the leading term in the size dependence of the diffusion constant

$$D_\alpha(M) \equiv D(M, j \ll M) \approx \gamma \left[\frac{M^{1-\alpha}-1}{1-\alpha} + O(M^{-\alpha}) \right] \tag{2.10}$$

for $\alpha<1$, and

$$D_1(M,j) \approx \gamma \left\{ C + \frac{1}{2}[\Psi(M-j+1)+\Psi(M+j+1)] \right\}, \tag{2.11}$$

for the critical value $\alpha=1$, where $C=0.577\ldots$ is Euler's constant and $\Psi(x)$ is the digamma function [23]. From this expression, it easily follows that

$$D_1(M) \approx \gamma \left[\ln(M+1) + C - \frac{1}{2(M+1)} \right]. \tag{2.12}$$

The logarithm is also obtained by taking the $\alpha \to 1^-$ limit in Eq. (2.10). As expected, these expressions diverge when $M \to \infty$. Note, in particular, that $D_0(M,j)=\gamma M$ for all j.

In the normal diffusion region, $\alpha>1$, we can use Riemann's zeta function $\zeta(\alpha)$ to write

$$D_\alpha(M) \approx \gamma \left[\zeta(\alpha) + O\left(\frac{M^{-(\alpha-1)}}{\alpha-1} \right) \right], \tag{2.13}$$

which for large M reduces to the standard diffusion coefficient, $D=D_\alpha(\infty)=\gamma\zeta(\alpha)$. This expression exhibits the well-known divergence of the standard diffusion coefficient when $\alpha \to 1^+$:

$$D_{\alpha \to 1^+} = \gamma \left(C + \frac{1}{\alpha-1} \right). \tag{2.14}$$

We can now easily estimate the dependence of $\hat{t}_M$ with α and M for the second moment, by identifying it with the typical diffusion time over the $(2M+1)$-site lattice. We obtain $\hat{t}_M \sim M^2$ for $\alpha>1$ and $\hat{t}_M \sim (1-\alpha)(2\gamma)^{-1} M^{1+\alpha}$ for $\alpha<1$. For the borderline $\alpha=1$ case, $\hat{t}_M \sim M^2/\ln(M)$.

III. TNSM PREDICTIONS FOR LÉVY FLIGHTS

Tsallis and co-workers [16] considered one-dimensional diffusion along the x axis and sought the optimum one-jump distribution $p_q(x)$ associated with the generalized q entropy

$$S_q(p) = \frac{k_B}{q-1} \left\{ 1 - \int_{-\infty}^{\infty} d\left(\frac{x}{\sigma} \right) [\sigma p(x)]^q \right\}, \tag{3.1}$$

where k_B is Boltzmann's constant, q a real number, and σ a finite characteristic length. The entropy was optimized subject to the constraints

$$\int_{-\infty}^{\infty} p(x)\,dx = 1 \tag{3.2}$$

and

$$\langle x^2 \rangle_q \equiv \int_{-\infty}^{\infty} d\left(\frac{x}{\sigma} \right) x^2 [\sigma p(x)]^q = \sigma^2. \tag{3.3}$$

In the work of Tsallis and collaborators, only symmetric one-jump distributions were considered. Hence, $V=0$ and there is a single threshold at $\alpha=1$. Equation (3.2) is the usual normalization condition, while Eq. (3.3) is the condition for the finiteness of the q expectation value of the square displacement.

The method of Lagrange multipliers yields the optimum functional form for the single-step distribution, which has the form

$$p_q(x) = \frac{A(q)}{[1+B(q)x^2]^{1/(q-1)}}. \tag{3.4}$$

Considering this equation for large distances and associating x with its discrete counterpart k, we can find a relation between α and the corresponding value of q:

$$q = \frac{\alpha+4}{\alpha+2}. \tag{3.5}$$

The N-jump distribution, $P_\alpha(x,N)$, can be calculated by an N -fold convolution of the one-jump distribution, $p_\alpha(x) = p_q(x)$, with itself. Since $p_\alpha(x \to \infty) \sim |x|^{-(\alpha+2)}$, the generalized central limit theorem indicates that the corresponding N-jump distribution is given, in the large N limit, by $P_\alpha(x,N) \sim L_{\alpha+1}(N^{-1/(1+\alpha)}x)$, where

$$L_\mu(y) = \frac{1}{2\pi} \int_{-\infty}^{\infty} e^{i\omega y} e^{-|\omega|^\mu} d\omega \tag{3.6}$$

is a Lévy function [1,25,26]. Asymptotically, $L_\mu(y) \sim |y|^{-(\mu+1)}$.

The generalized Rth-displacement moment can be calculated as

$$\langle x^R(N) \rangle_q \equiv \int_{-\infty}^{\infty} d\left(\frac{x}{\sigma} \right) x^R [\sigma P_\alpha(x,N)]^q, \tag{3.7}$$

which yields

$$\langle x^R(N) \rangle_q = \sigma^{q-1} (C_\alpha N)^{[R(2+\alpha)-2]/[(\alpha+1)(\alpha+2)]} \times \int_{-\infty}^{\infty} dy\, y^R [L_{\alpha+1}(y)]^q, \tag{3.8}$$

where

$$C_\alpha = \frac{\pi \gamma_\alpha}{\Gamma(\alpha+2)\cos\left(\frac{\alpha\pi}{2} \right)}. \tag{3.9}$$

Here $\gamma_\alpha = \mathrm{Lim}(|x| \to \infty)\ |x|^{(\alpha+2)} p_\alpha(x)$ and $\Gamma(x)$ is the usual gamma function [23].

From these equations we see that the generalized moments have the following properties.

(a) They are finite only if

$$\alpha > R-3 \tag{3.10}$$

(a simple calculation shows that the conventional moments are finite if $\alpha > R-1$). Of course, normalization always requires $\alpha > -1$. Note that the generalized zeroth order moment ($R=0$) does not coincide with the probability normalization.

(b) If $R=2$, we recover the result due to Tsallis and coworkers [16], $\langle x^2(N)\rangle_q \sim N^{2/(2+\alpha)}$.

(c) If $R>2/3$, they have a power law singularity when $\alpha \to 1^-$

$$\langle x^R(N)\rangle_q \sim (1-\alpha)^{(2-3R)/6}. \tag{3.11}$$

This singularity gets stronger for higher moments.

(d) If α decreases, q increases and $[P_\alpha(x,N)]^q$ decreases faster with x for large x. For this reason, we expect the generalized moments to be increasing functions of α. A detailed curve for the $R=2$ moment and large N is shown in Ref. [16].

(e) We stress that Eq. (3.8) is valid only in the $N \to \infty$ limit. The generalized central limit theorem says nothing about the behavior of $P_\alpha(x,N)$ for small and intermediate values of N. To obtain information in that case a simulation is required.

IV. NUMERICAL RESULTS AND DISCUSSION

Two methods were used for the numerical evaluation of the moments: The first was a direct time discretization of the master equation. The time-discretized form of Eq. (2.1) for symmetric flights in the lattice $[-M,M]$ and *reflecting* (in the sense defined above) BC's is given by

$$P_j(t+\tau) = P_j(t) + \tau \left\{ \sum_{k=1}^{M-j} \Gamma_k [P_{j+k}(t) - P_j(t)] + \sum_{k=1}^{M+j} \Gamma_k [P_{j+k}(t) - P_j(t)] \right\}, \tag{4.1}$$

where τ is the time-discretization interval length. The second and third terms on the right-hand side stand for jumps to and from the right and the left of site j, respectively. We remark that, for the sake of clarity, we are using slightly different notations for the continuum distribution and its lattice counterpart. The correspondence is defined through $p(x) \leftrightarrow \Gamma_j$ and $P_\alpha(x,N) \leftrightarrow P_j(N)$ [or $P_j(t)$].

For *absorbing* BC's, we can embed the lattice in a much bigger one (thus relaxing the upper limits of the sums) and fix $P_j=0$ at each step $\forall j/|j|>M$. The time-discretized iteration equation is

$$P_j(t+\tau) = P_j(t) + \tau \sum_{k=1}^{M+j} \Gamma_k [P_{j-k}(t)\Theta_{j-k+M} + P_{j+k}(t)\Theta_{M-j-k} - 2P_j(t)], \tag{4.2}$$

where Θ_x is Heaviside step function.

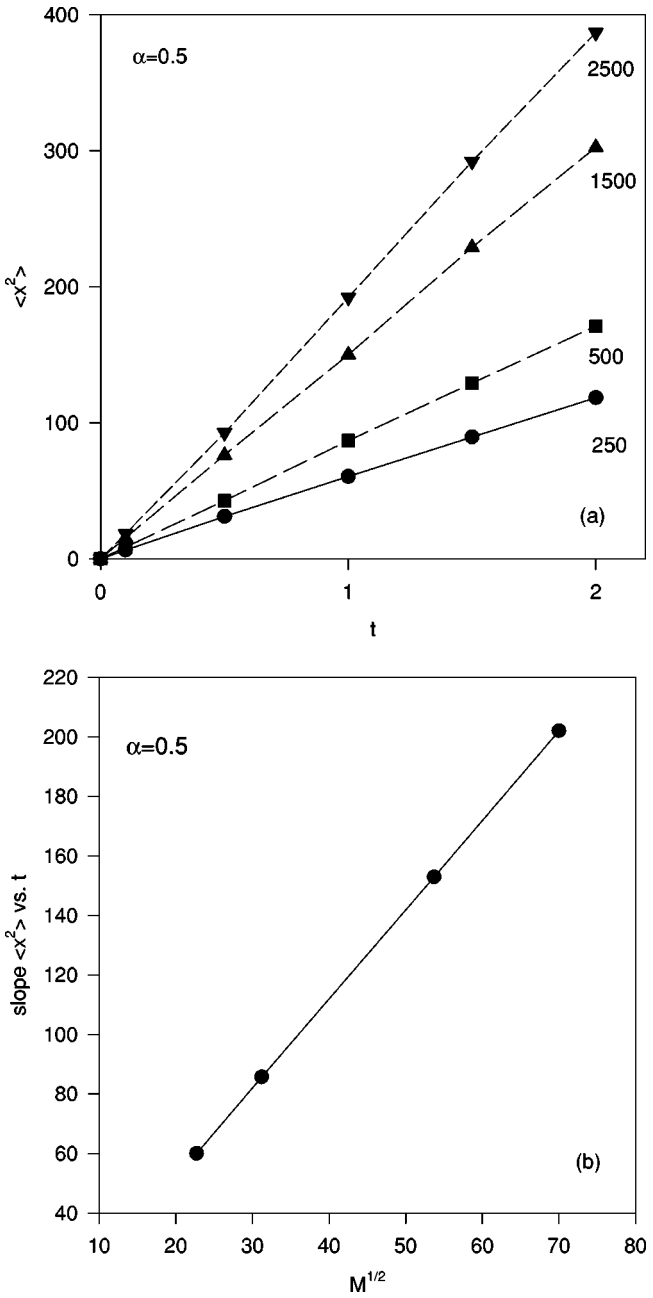

FIG. 1. (a) Time dependence (a.u.) of the standard mean-square displacement for $\alpha=0.5$ ($q=1.8$) on the lattice sizes as indicated in the figure. (b) Slopes of the straight lines in (a) as functions of $M^{1-\alpha}=M^{1/2}$.

The second method was a Monte Carlo simulation. Instead of starting from a master equation, we divided the interval (0,1) in juxtaposed "windows" whose widths W_k are proportional to the jump probabilities for jumps of length k. For large M we can take, to a good approximation,

$$W_k = \frac{1}{2k^{a+2}} \left(\sum_{j=1}^{\infty} \frac{1}{j^{a+2}} \right)^{-1}. \tag{4.3}$$

Next, a number is chosen at random in the interval (0,1). The length of the resulting jump depends on the window the

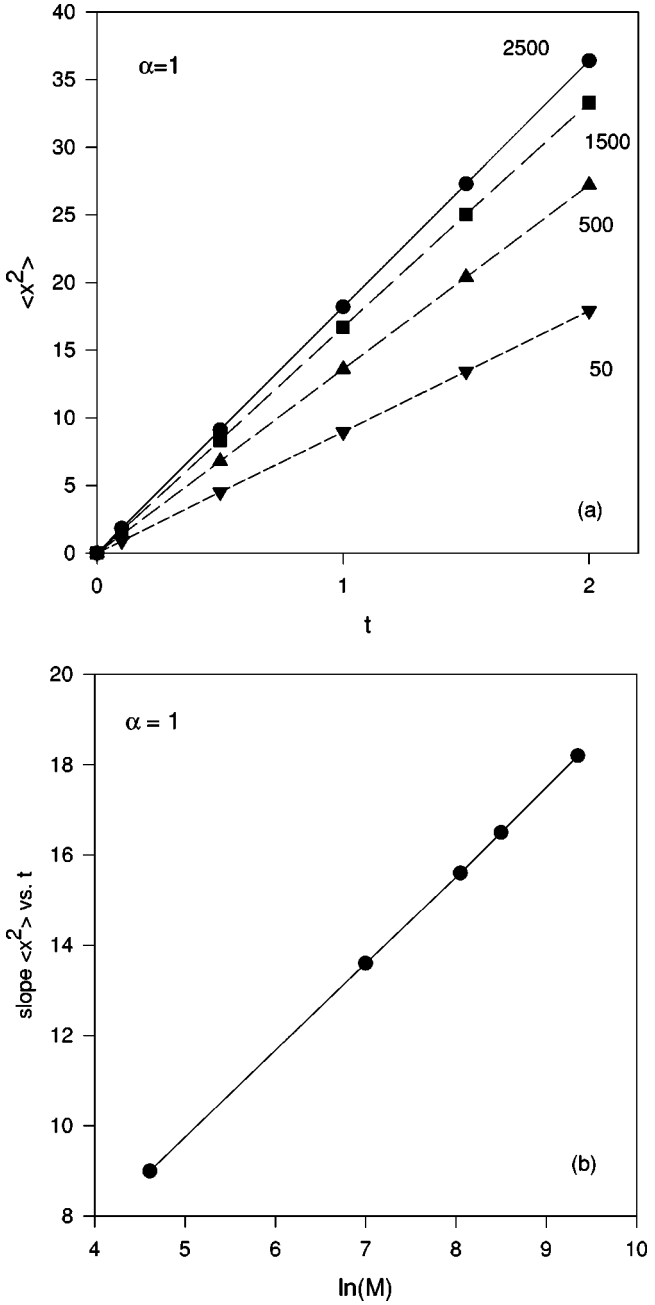

FIG. 2. (a) Time dependence (a.u.) of the standard mean-square displacement for $\alpha=1$ $(q=5/3)$ on the lattice sizes as indicated on the figure. (b) Slopes of the straight lines in (a) as functions of $\ln(M)$.

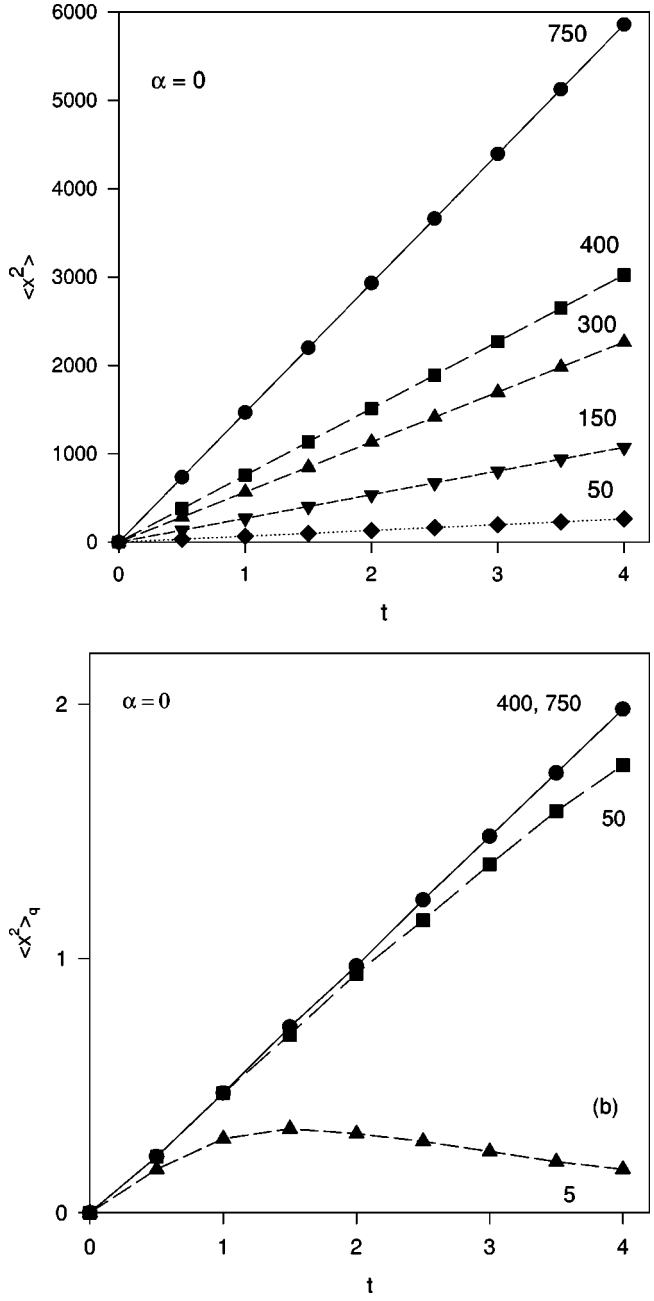

FIG. 3. Mean square displacement as a function of time for $\alpha=0$ $(q=2)$ and the lattice sizes indicated on the figure. (a) Standard MSD: the slope increases monotonically with lattice size. (b) Generalized MSD: the curves converge to a finite-slope straight line. Note that the slopes for the cases $M=400$ and $M=750$ are indistinguishable.

selected number falls into. A new random number is now chosen, which determines the length of the second jump (this jump starts from the new position). After repeating N times the process we obtain the final position for the particle in one particular experiment. By repeating the experiment a large number of times we obtain a histogram that provides us with the distribution $P_j(N)$.

Some remarks are in order.

(a) Since each site is connected to each other site at each time step, it is easy to see that the required number of operations (and thus the computation time) for a given step number increases with lattice size as M^2.

(b) While for reflecting BC's the probability is conserved, for absorbing BC's we must compute the displacement moments considering only the contribution of the *surviving* particles.

(c) We have used both reflecting and absorbing BC's, obtaining consistent results.

(d) The results obtained by the ''master equation'' and Monte Carlo methods can be compared by setting $t=N\tau$. Their reliability was guaranteed by comparing them and de-

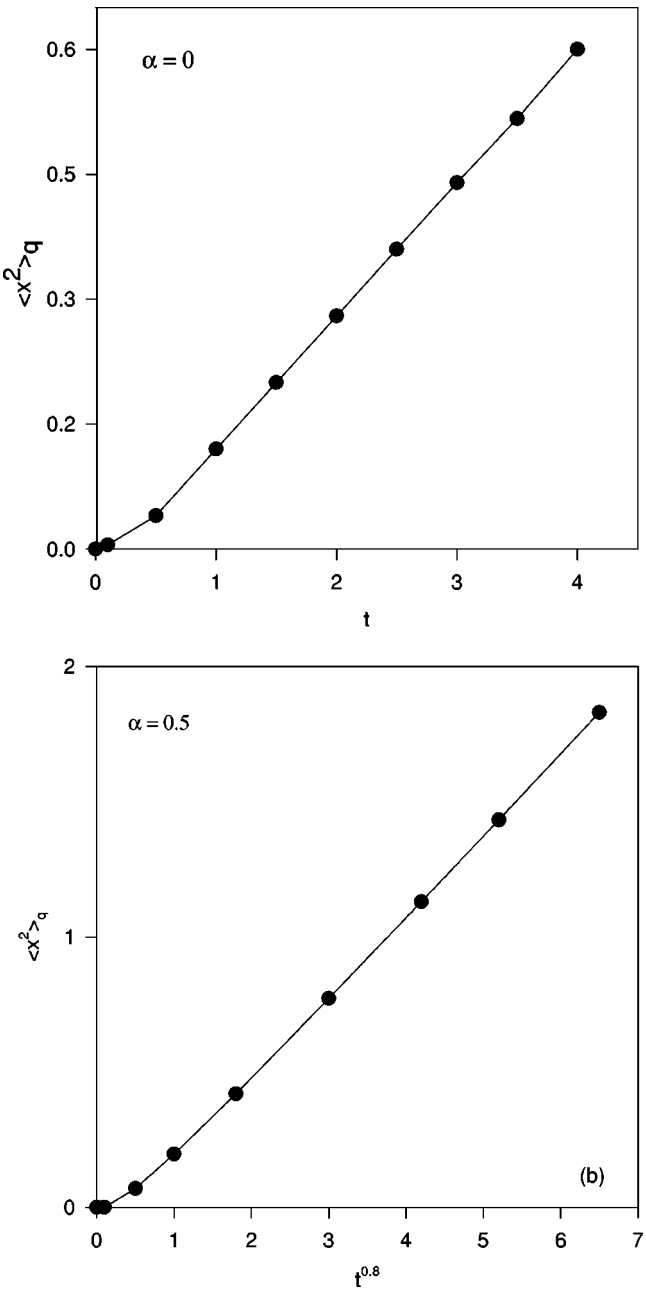

FIG. 4. Generalized MSD as a function of $t^{2/(2+\alpha)}$. Here $M=2500$, and we have iterated the master equation 1000 times. (a) $\alpha=0$ $(q=2)$; (b) $\alpha=0.5$ $(q=1.8)$. The slopes are, respectively, 0.1537 and 0.296.

manding close agreement. The choice $\tau=0.01$ proved to be appropriate in all cases considered.

Once the probability distribution is known, the generalized mean square displacement is calculated as

$$\langle x^2(t)\rangle_q = \frac{\sum_{j=-M}^{M} j^2 [P_j(t)]^q}{\sum_{j=-M}^{M} P_j(t)}. \tag{4.4}$$

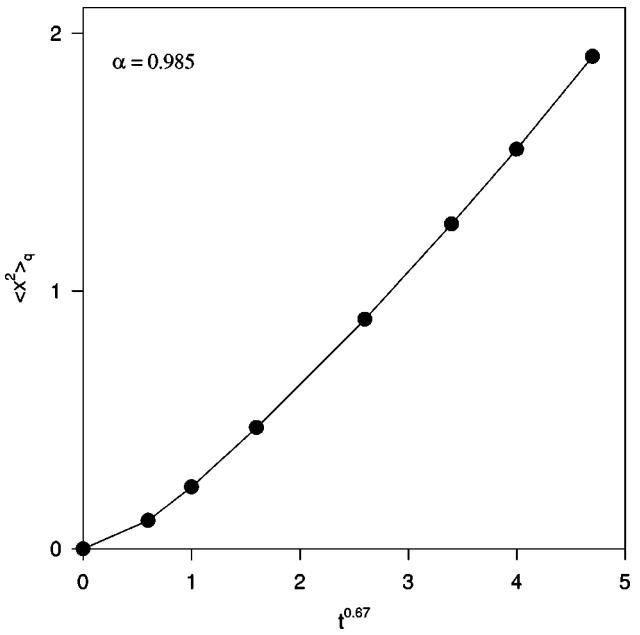

FIG. 5. Generalized MSD as a function of $t^{2/(2+\alpha)}$ for $\alpha=0.985$ $(q=1.67)$. Here $M=2500$, $\tau=0.01$ and we have iterated the master equation 1000 times. The slope increases continuously.

The denominator is automatically equal to unity in the case of reflecting BC's.

First, we look at finite-size effects. According to Eqs. (2.10) and (2.12), the effective diffusion coefficient should have a simple dependence on the lattice size. To verify this, we have calculated the slope of the standard mean-square displacement (SMSD) as a function of time for several values of M. The results are depicted in Figs. 1 and 2 for $\alpha=0.5$ and $\alpha=1$, respectively. They show that the SMSD grows linearly with time in all cases, with a slope that increases monotonically with the lattice size. For an infinite-size lattice the slope would diverge. Figures 1(b) and 2(b) confirm that the dependence of the slopes on the lattice size is accurately predicted by Eqs. (2.10) and (2.12).

The dependence of the generalized mean-square displacement (GMSD) on lattice size is shown in Fig. 3, where we chose $\alpha=0$. Upon increasing M, the curves giving the GMSD converge to a finite-slope straight line. This should be compared to the rapid increase in the SMSD slope, as evidenced by Fig. 3(a). The dependence on α is shown in Fig. 4, where the GMSD is plotted against $t^{2/(2+\alpha)}$ for $\alpha=0$ and $\alpha=0.5$. Apparently, straight lines with well-defined slopes result, in agreement with the predictions of Ref. [16] for the dependence on jump number. However, while the slope in Fig. 4(a) coincides precisely with the predictions, the slope in Fig. 4(b) turns out to be about 10% too small (0.296 against 0.331). The differences increase as we let $\alpha\to 1^-$. Indeed, in Fig. 5 we see that, for a value of α close to unity, the average slope does not grow as $(1-\alpha)^{-2/3}$, as predicted by the large N theory. A closer look reveals that the slope in Fig. 5 is slowly increasing at all times considered.

What is the reason for this disagreement? It is unlikely that it is due to the difference between diffusion on a continuum and on a discrete lattice; the qualitative properties of

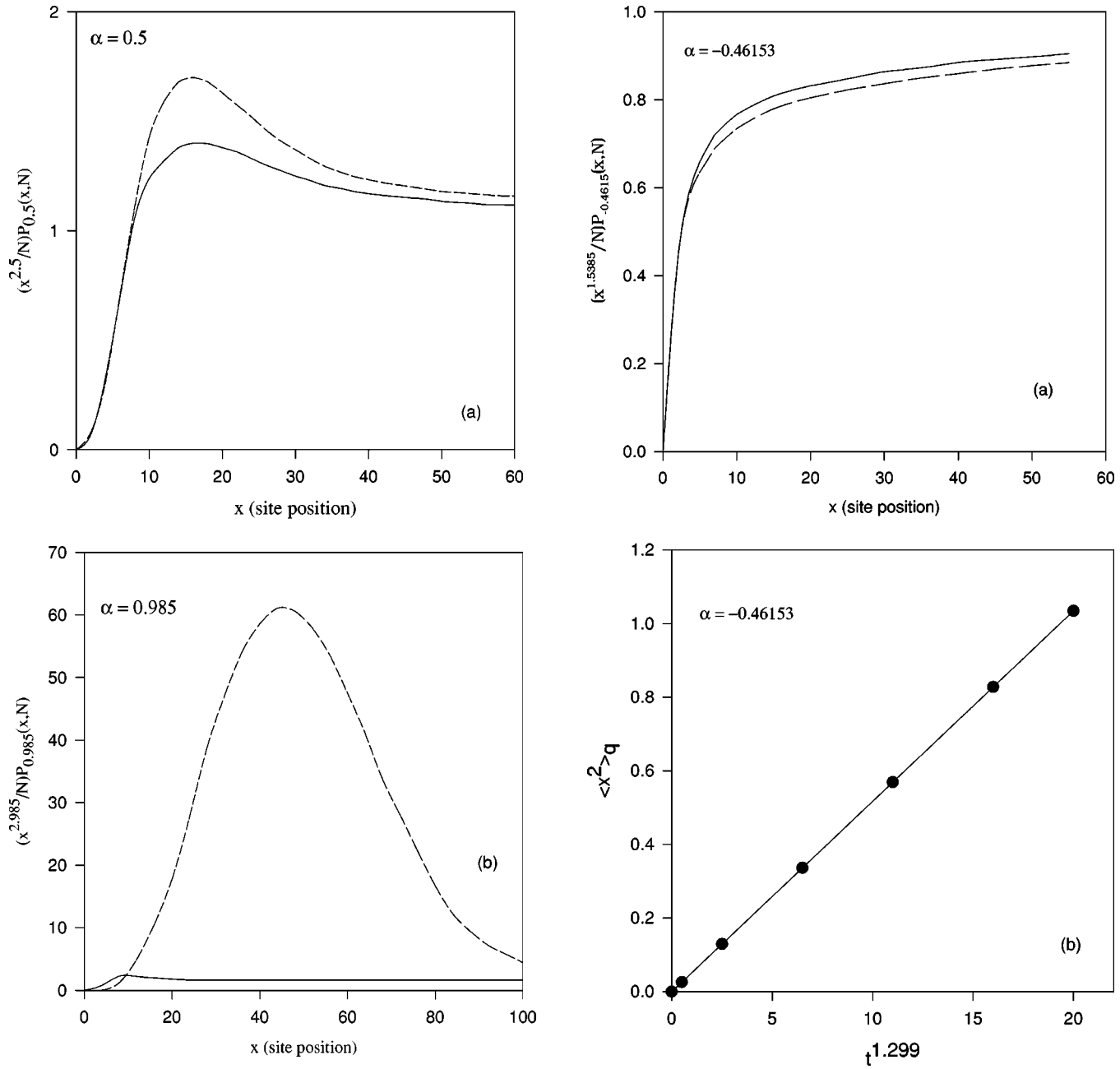

FIG. 6. *Master equation* results for the asymptotic (dashed lines) and finite-time distributions as functions of the lattice position. (a) $\alpha=0.5$ ($q=1.8$); (b) $\alpha=0.985$ ($q=1.67$). In both cases, $N=500$ jumps.

FIG. 7. The case $\alpha=-0.4615$ ($q=2.3$). (a) Comparison between the analytical asymptotic (dashed line) and simulation (solid line) distributions for $N=30$. (b) Generalized MSD as a function of $t^{2/(2+\alpha)}$. Here we took $M=10\,000$ and performed up to 1000 iterations using the master equation.

the system are controlled by long jumps, for which no substantial differences can arise between the continuum and the discrete cases. The excellent agreement obtained for $\alpha=0$ and the progressive disagreement obtained as we move away from this case suggest a different explanation. If $\alpha=0$ our starting jump distribution is a discretized form of the Cauchy distribution, which is a stable law. Consequently, the system is already at a fixed point at the start of its evolution. As $|\alpha|$ grows, the starting distribution differs more and more from a Lévy distribution: the beginning point is then further away in the corresponding attraction basin. Therefore, it takes the representative point longer and longer to reach the attractor neighborhood. It is this neighborhood that corresponds to the asymptotic regime, for which the generalized central limit theorem holds.

To back the preceding explanation, we examined the probability distributions themselves and compared the predictions of the asymptotic theory (i.e., those resulting from the central limit theorem) [17] with the results of the simulations. In Fig. 6 we compare the numerical and the (analytical) asymptotic distributions for two values of α and $N=500$. In order to enhance the differences, we have actu-

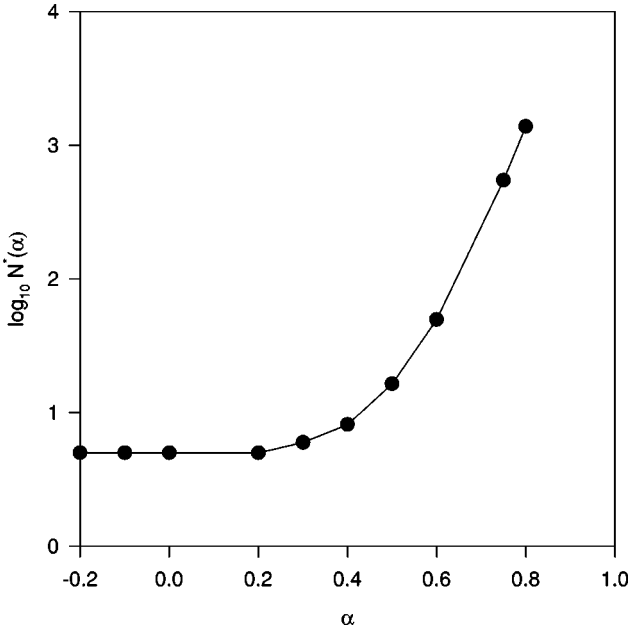

FIG. 8. Number of Monte Carlo iterations required for the generalized MSD to converge to within 10% of the asymptotic theory as a function of α. Each point was obtained by averaging the results of 10^6 experiments on an $M=5000$ lattice.

ally plotted the function $(x^{2+\alpha}/N)P_\alpha(x,N)$. In all cases these curves tend to unity for large x. This asymptotic form is responsible for the agreement between numerical and analytical results for the large N (or large t) dependence. However, we also observe that the intermediate-times maximum is higher for the analytical case (much higher if $\alpha=0.985$). The presence of this spuriously high maximum indicates the lack of applicability of the asymptotic theory for intermediate times in the $\alpha\to 1^-$ region. A plot (not shown here) for the $\alpha=0$ case shows that the numerical curve falls almost exactly on the asymptotic curve, as expected, confirming that in the $\alpha\approx 0$ neighborhood the asymptotic theory works well even at short times.

A further argument is provided by a look at the $\alpha>1$ region. According to the ordinary central limit theorem, the Gaussian $G(x)$ is the attractor for all these distributions. However, the number of steps needed to reach the attractor neighborhood depends strongly on α. This dependence can be seen from Chebyshev's theorem, which reads [1,25]

$$\int_{-\infty}^{Z}[P(x,N)-G(x)]dx=\frac{1}{2\pi}e^{-Z^2}\sum_{j=1}^{\infty}\frac{Q_j(Z)}{N^{j/2}}, \quad (4.5)$$

where P is in the Gaussian basin and the $Q_j(Z)'s$ are polynomials in Z whose coefficients involve integer moments of x . Since these moments increase if α decreases, higher values of N will be required to keep the left-hand side of Eq. (4.5) under a given bound. Therefore, the convergence slows down as α decreases, i.e., as the average jump length increases. Our runs in the region $\alpha>1$ confirm this behavior.

Because they require the use of larger lattices, reliable intermediate-time simulations in the $\alpha<0$ regime demand more computer power. The apparent lack of an intermediate x "hump" in the function $(x^{2+\alpha})L_{\alpha+1}(x)$ suggests that the analytical asymptotic results should also hold at finite times. We have performed runs for $\alpha=-0.4615$ $(q=2.3)$ and the results are presented in Fig. 7. There we see that a 30-step simulation already yields very good agreement with the asymptotic curve. It is, therefore, not surprising that the GMSD data fall almost exactly on a straight line when plotted against $t^{2/(2+\alpha)}$ [see Fig. 7(b)].

We stated that, as α grows, it takes the representative point longer and longer to reach the attractor neighborhood. This is clearly seen in Fig. 8, where we have plotted the number of iterations $N^*(\alpha)$ required for the generalized mean-square displacement to converge to within 10% of the asymptotic theory as a function of α. Up to $\alpha=0.2$ the required number of iterations is small, growing very slowly as a function of α. Starting from $\alpha\sim 0.2$, it begins to grow faster and faster, and it is likely to diverge as $\alpha\to 1^-$.

V. CONCLUSIONS

We investigated some properties of the displacement moments for Lévy flights on lattices. For finite lattices, we obtained the dependence of the diffusion coefficient on lattice size; for infinite lattices, the standard displacement moments in the anomalous region are not defined and we examined the problem under the light of the approach introduced by Tsallis and collaborators. The properties of the generalized displacement moments were discussed and then simulations were performed in order to obtain their short- and medium-time (or jump number) behavior.

We believe that further mathematical work is needed to fully understand the finite-time properties of Lévy flights, as well as to relate the properties of continuum and discrete flights. Our numerical results suggest that, if experimental systems are shown to be describable in terms of generalized displacement moments for Lévy flights, the robust $N^{2/(2+\alpha)}$ (or $t^{2/(2+\alpha)}$) dependence of the exponent should be approximately observed over a large portion of the anomalous range. The detailed α dependence of the coefficient predicted by the asymptotic theory should, on the other hand, occur only in the neighborhood of $\alpha=0$. The size of this neighborhood should increase as the experiment probes longer and longer times.

ACKNOWLEDGMENTS

This research was supported by the NSF through Grant No. HRD-9450342 and by a grant from Fundación Antorchas. The authors are grateful to C. Tsallis for his continuous encouragement, and to Silvio Levy and D.P Prato for useful correspondence and discussions, respectively. We also wish to thank I. Delgado for help with the computations.

[1] See, for example, J.P. Bouchaud and A. Georges, Phys. Rep. **195**, 127 (1990), and references therein.
[2] A. Ott, J.P. Bouchaud, D. Langevin, and W. Urbach, Phys. Rev. Lett. **65**, 2201 (1990).
[3] M.F. Shlesinger, G.M. Zaslavsky, and J. Klafter, Nature (London) **363**, 31 (1993).
[4] S.V. Buldyrev *et al.*, Phys. Rev. E **47**, 4514 (1993).
[5] J. Klafter, M.F. Shlesinger, and G. Zumofen, Phys. Today **49** (2), 33 (1996).
[6] E.R. Weeks, J.S. Urbach, and H.L. Swinney, Physica D **97**, 291 (1996).
[7] E.R. Weeks and H.L. Swinney, Phys. Rev. E **57**, 4915 (1998).
[8] G.M. Viswanathan, V. Afanasyev, S.V. Buldyrev, E.J. Murphy, P.A. Prince, and H.E. Stanley, Nature (London) **381**, 413 (1996).
[9] P. Santini, Phys. Rev. E **61**, 93 (2000).
[10] R. Metzler and J. Klafter, Phys. Rep. **339**, 1 (2000).
[11] L. Couto Miranda and R. Riera, Physica A **297**, 509 (2001).
[12] G.M. Viswanathan, S.V. Buldyrev, S. Havlin, M.G.E. da Luz, E.P. Raposo, and H.E. Stanley, Nature (London) **401**, 911 (1999).
[13] G.M. Viswanathan, V. Afanasyev, S.V. Buldyrev, S. Havlin, M.G.E. da Luz, E.P. Raposo, and H.E. Stanley, Physica A **282**, 1 (2000).
[14] G.M. Viswanathan, V. Afanasyev, S.V. Buldyrev, S. Havlin, M.G.E. da Luz, E.P. Raposo, and H.E. Stanley, Physica A **295**, 85 (2001).
[15] D.H. Zanette and P.A. Alemany, Phys. Rev. Lett. **75**, 366 (1995).
[16] C. Tsallis, S.V.F. Levy, A.M.C. Souza, and R. Maynard, Phys. Rev. Lett. **75**, 3589 (1995); **77**, 5442 (1996).
[17] C. Tsallis, A.M.C. de Souza, and R. Maynard, in *Levy Flights and Related Phenomena in Physics*, edited by M.F. Shlesinger, U. Frisch, and G.M. Zaslavsky (Springer, Berlin, 1995).
[18] C. Tsallis, J. Stat. Phys. **52**, 479 (1988).
[19] C. Tsallis, Braz. J. Phys. **29**, 1 (1999).
[20] D.H. Zanette, Braz. J. Phys. **29**, 108 (1999).
[21] See, for example, the papers quoted in Refs. [16,17,19,20]. An updated bibliography is accessible at http://tsallis.cat.cbpf.br/biblio.htm.
[22] See, however, M.L. Lyra, and C. Tsallis, Phys. Rev. Lett. **80**, 53 (1998). This paper presents a relationship between q and the properties of the attractor multifractal singularity spectrum in a low-dimensional dissipative system.
[23] M. Abramowitz and I. Stegun, *Handbook of Mathematical Functions* (Dover, New York, 1972), p. 807.
[24] R.N. Mantegna and H.E. Stanley, Phys. Rev. Lett. **73**, 2946 (1994).
[25] B.V. Gnedenko and A.N. Kolmogorov, *Limit Distributions for Sums of Independent Random Variables* (Addison-Wesley, Reading, MA, 1954).
[26] R.G. Laha and V.K. Rohatgi, *Probability Theory* (Wiley, New York, 1979).